

# A novel SIMIDCBC topology driven PMSM for PEV application

Chinta Anil Kumar<sup>1</sup>, Kandasamy Jothinathan<sup>1</sup>, Lingineni Shanmukha Rao<sup>2</sup>

<sup>1</sup>Department of Electrical and Electronics Engineering, Faculty of Engineering and Technology, Annamalai University, Chidambaram, Tamilnadu, India

<sup>2</sup>Department of Electrical and Electronics Engineering, Kallam Haranadhareddy Institute of Technology, Guntur, India

## Article Info

### Article history:

Received Mar 9, 2023

Revised Jun 10, 2023

Accepted Jun 24, 2023

### Keywords:

Battery energy storage system

Multi-input boost converter

Plug-in electric vehicles

PM synchronous motor

Renewable energy sources

Switched inductors

## ABSTRACT

Nowadays, the usage of renewable energy based electric vehicles is increased for reducing CO2 emissions, usage of fossil fuels, energy saving, and transportation cost. As a result, it becomes the most significantly run with combined energy sources and it is good choice which minimizes the energy consumption from charging stations. The available renewable energy is integrated to power-train through power-electronic interface; such interface consists of three-phase inverter with DC-DC boost converter. The combined energy sources like solar-PV/battery are integrated to power-train by employing multi-input non-isolated step-up DC-DC converter for providing continuous power to drive the vehicle. The multi-terminal topologies have efficient, reliable performance, continuous input current, high step-up gain over the conventional DC-DC converters. In this work, a unique framework of combined energy powered switched-inductor based multi-input DC boost converter topology has been proposed to drive the PMSM. The performance of proposed SIMIDCBC topology driven PMSM for PEV application under constant and variable speed conditions are verified by using MATLAB/Simulink tool, simulation results are presented.

*This is an open access article under the [CC BY-SA](https://creativecommons.org/licenses/by-sa/4.0/) license.*



## Corresponding Author:

Chinta Anil Kumar

Department of Electrical and Electronics Engineering, Faculty of Engineering and Technology

Annamalai University

Annamalai Nagar, Chidambaram, Tamil Nadu 608002, India

Email: chanilkumar.eee@gmail.com

## 1. INTRODUCTION

In India, more than 35% of population utilizes the plug-in EV's such as electric bike; electric auto and e-bicycle which are rapidly increased to balance the global fuel prices [1]–[3]. In general, all these vehicles are run by batteries which are charged through utility-grid powered charging stations and cause the system loss due to proliferation of power-quality. The charging station consists of non-linear devices, which distorts the main supply current by injecting the harmonic current distortions and also affecting the voltage profile of utility-grid [4]. A substantial energy source has been adopted to establish the required power demand to drive EV system and also it reduces the crucial problems on utility grid [5], [6]. On sincere attempts, all over the world utilizes the renewable energy sources (RES) for sustainable energy production, social development, more efficient and economical. Amid, the solar-PV is the most recognized and viable for EV system because of eco-friendly, non-toxic, ample nature, virtuous, and more economical [7]. However, it can produce 30% of more power over the conventional diesel or petrol operated vehicles. The available renewable energy is integrated to electric motor through power-electronic interface; such interface consists of voltage-source inverter (VSI) with DC-DC boost converter [8].

In this regard, PMSM has immense popularity because of simple/light weight structure, robustness, wide speed range, high overload capacity, easy control due to its low inertia rotor, high torque-inertia ratio, reliable performance, less noise, and more efficiency over the BLDC motor [9]. The solar-PV powered PMSM drive is controlled through VSI for obtaining the variable speeds at different torque regions [10]. But, the use of individual solar-PV is not worthy because of discontinuous power flow during varying temperature and irradiation conditions. Thus, the combined energy generation is the most suitable to maintain continuous power flow to PMSM drive with the help of battery energy storage (BES) unit. The solar-PV with BES unit is act as combined source for energizing the PMSM motor through high step-up DC-DC converter. It acts as power conditioning device, converts available solar-PV/BES voltage into constant high step-up DC voltage to drive the PMSM drive [11], [12]. The traditional single-input DC-DC boost converters (SIDCBCs) configuration is depicted in Figure 1. It is not preferable for interfacing these solar-PV/BES units by virtue of unreliable, complicate structure and influences the compactness of EV system.

To overcome these problems in traditional SIDCBC structure, a multi-input DC-DC boost converters (MIDCBC's) structure is the significant choice and have reliable, simple and easy control function. From the various literature reviews, the feasible MIDCBCs structure is classified as non-isolated and isolated design, bidirectional, and unidirectional power-flow type converters, have its own merits and demerits. The proposed multi-input DC-DC boost converter (MIDCBCs) configuration is depicted in Figure 2. A widespread generic approaches for synthesis of several MIDCBC's are presented in [13]. A two-port interleaved boost topology with low step-up gain is highlighted in [14]. A multi-port bidirectional DC-DC converter with positive output voltage is developed in [15].

A multi-terminal DC-DC topology is proposed in [16], it can operate in both buck and boost operations with an extra storage capacity which maximizes the cost, size, structure and reducing the overall efficiency of the system. The novel MIDCBC's configuration is explored [17], for micro-grid powered telecom devices which attains high efficiency [18], although it necessitates the more storage units. An inventive approach for developing the multi-port DC-DC topology with a high step-up conversion ratio is highlighted in [19], however it doesn't require any electrolytic capacitors for maximizing the reliability of topology. A coordinated input sources with multi-port DC-DC SEPIC converter topology is explored in [20], [21].

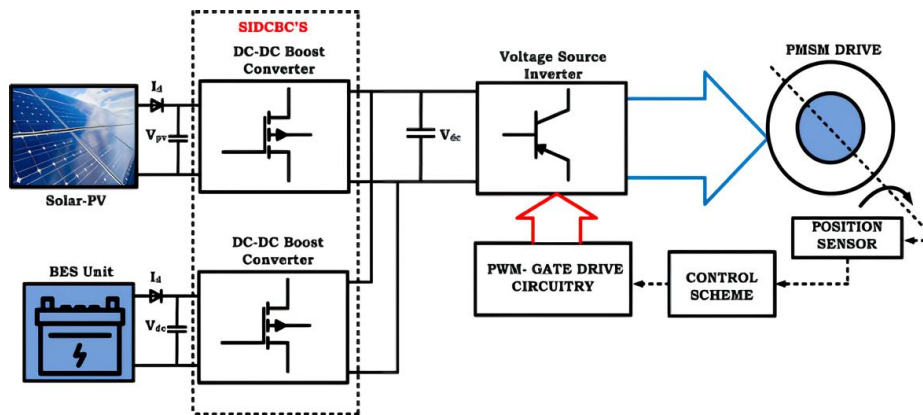


Figure 1. Block diagram of traditional SIDCBC structure

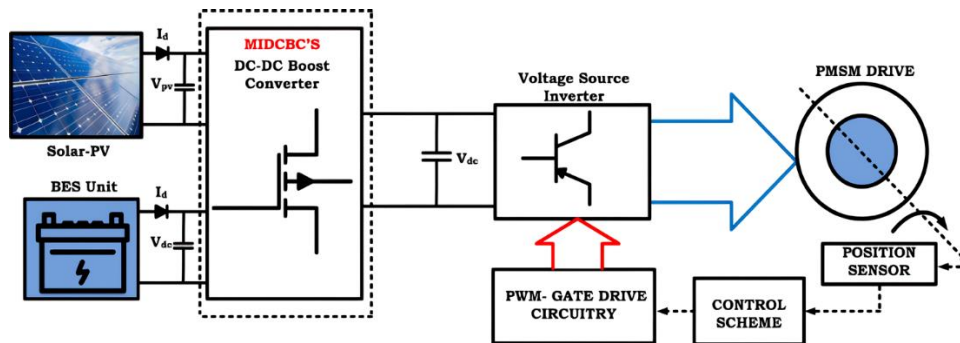


Figure 2. Block diagram of proposed MIDCBC structure

A novel configuration of multi-input converter with bidirectional power-flow functioned in buck and boost operations with low conversion ratio is presented in [22]. Babaei and Abbasi in [23], new multi terminal input and output DC-DC boost topology is presented, although it is inefficient because of increased number of switching elements with boosting the output voltage as 3 times of input voltage. A new DC-DC three-port converter is connected to a standalone R-load by using three individual input sources, it boosts the output voltage as 4 times of input voltage is investigated in [24]. However, because this design has more switching elements, the converter topology and its control unit are more complicated. For achieving the high step-up voltage, the individual inductors are replaced with switched inductor which are controlled through specific switching pattern which produces the boost voltage as 5 times of input voltage is proposed in [25], [26]. However, the major problem in these multi-input converters for obtaining constant DC-link voltage with boost competency are clearly highlighted by many researchers.

The main contribution of this work is designing the novel MIDCBC converter by utilizing the switched-inductors for getting high voltage gain. In this work, a novel switched-inductor based multi-input DC-DC boost (SIMIDCBC) converter topology has been proposed for obtaining high boost voltage along with simple design and reduced switching elements which is operated in a continuous conduction mode (CCM) for attaining the wide conversion voltage ratio's. The performance of proposed SIMIDCBC topology driven PMSM for PEV application under constant and variable speed condition is verified by using MATLAB/Simulink tool, simulation results are presented.

## 2. PROPOSED METHOD

The schematic diagram of proposed SIMIDCBC topology driven PMSM for PEV application is shown in Figure 3. It consists of various components such as dual input DC sources which are considered as solar-PV and BESS unit, proposed SIMIDCBC topology, VSI structure, PMSM drive, sinusoidal pulse-width modulation (SPWM), proportional-integral (PI) controller, respectively. The switching operation of proposed SIMIDCBC topology is explained clearly in detail. The proposed SIMIDCBC is powered by dual input DC sources with a input voltage of  $V_{in1}$ ,  $V_{in2}$ , and input current of  $I_{in1}$ ,  $I_{in2}$  to drive the PMSM drive load. It comprises of two supply controlled switches named as  $S_{s1}$ ,  $S_{s2}$  with diodes  $D_{s1}$ ,  $D_{s2}$ , and one monitoring switch named as  $S_{sm}$  for controlling the switching action of SIMIDCBC topology to achieve high boost voltage competency. However, it consists of two switched-inductor cells, in first cell inductors  $L_{a1}$ ,  $L_{a2}$  are connected with diodes  $D_{a1}$ ,  $D_{a2}$ ,  $D_{a3}$  which is integrated to the positive polarity of input DC supply. The second cell is the exact replica of first cell, the inductors  $L_{b1}$ ,  $L_{b2}$  are connected with diodes  $D_{b1}$ ,  $D_{b2}$ ,  $D_{b3}$ , which is integrated to the negative polarity of input DC supply. The high boost voltage competency is obtained at load terminals by proper switching of switched-inductor cells based on parallel charging and series discharging by turn ON/OFF of the switches  $S_{s1}$ ,  $S_{s2}$ , and  $S_{sm}$ , periodically. Also, diode  $D_o$  is output diode while the DC-link capacitor  $C_o$  serves the load when output diode  $D_o$  is in reverse-bias mode. The schematic diagram of proposed SIMIDCBC topology is shown in Figure 4.

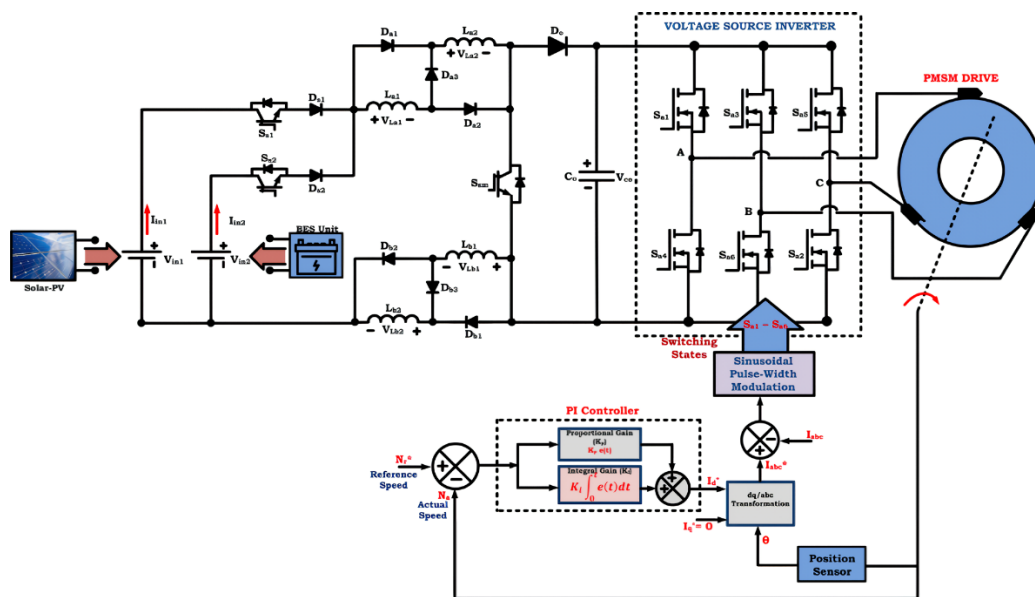


Figure 3. Schematic diagram of proposed SIMIDCBC topology driven PMSM for PEV application

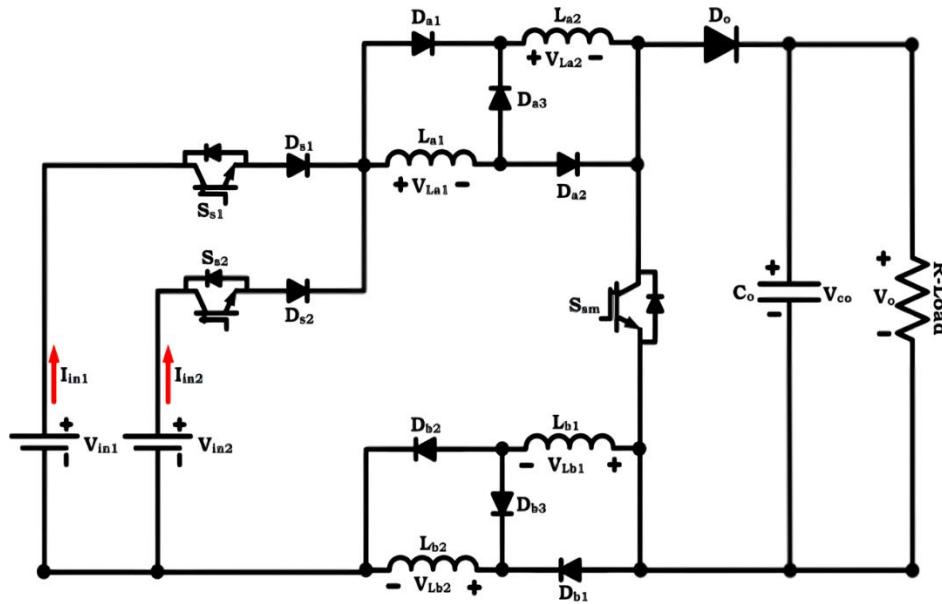


Figure 4. Schematic diagram of proposed SIMIDCBC topology

## 2.1. Operating modes

The operating modes of proposed SIMIDCBC topology is shown in Figure 5.

- Mode-1 ( $t_0$ - $t_1$ ): In this mode, the two switches  $S_{s1}$  and  $S_{sm}$  are turned-ON together by providing the switching pulses through SPWM circuitry. The input voltage  $V_{in1}$  energizes the both switched inductor cells, the inductors in first cell  $L_{a1}$ ,  $L_{a2}$  is charging and also store's energy towards the input voltage  $V_{in1}$  through switches  $S_{s1}$ ,  $S_{sm}$  along with diodes  $D_{a1}$  and  $D_{a2}$ . Also, the inductors in second cell  $L_{b1}$ ,  $L_{b2}$  is charging and also store's energy towards the input voltage  $V_{in1}$  through switches  $S_{s1}$ ,  $S_{sm}$  along with diodes  $D_{b1}$  and  $D_{b2}$ . Accordingly, the input current  $I_{in1}$  flows continuously in both switched inductor cells and increased linearly, then the output diode  $D_o$  is in reverse bias to make parallel charging of switched-inductor cells. Thus, the DC-link capacitor discharges energy to load and meets the load requirement until switch  $S_{s1}$  comes to turned-OFF. The mode-1 operation of SIMIDCBC topology is shwon in Figure 5(a).
- Mode-2 ( $t_1$ - $t_2$ ): In this mode, the two switches  $S_{s2}$  and  $S_{sm}$  are turned-ON together by providing the switching pulses through SPWM circuitry. The input voltage  $V_{in2}$  energizes the both switched inductor cells, the inductors in first cell  $L_{a1}$ ,  $L_{a2}$  are charging and also store's energy towards the input voltage  $V_{in2}$  through switches  $S_{s2}$ ,  $S_{sm}$  along with diodes  $D_{a1}$  and  $D_{a2}$ . Also, the inductors in second cell  $L_{b1}$ ,  $L_{b2}$  are charging and also store's energy towards the input voltage  $V_{in2}$  through switches  $S_{s2}$ ,  $S_{sm}$  along with diodes  $D_{b1}$  and  $D_{b2}$ . Accordingly, the input current  $I_{in2}$  flows continuously in both switched inductor cells and increased linearly, then the output diode  $D_o$  is in reverse bias to make parallel charging of switched-inductor cells. Thus, the DC-link capacitor discharges energy to load and meets the load requirement until switch  $S_{s2}$  comes to turned-OFF. The mode-2 operation of SIMIDCBC topology is shwon in Figure 5(b).
- Mode-3 ( $t_1$ - $t_3$ ): In this mode, the one switch  $S_{s2}$  is turned-ON by providing the switching pulse through SPWM circuitry and then the monitor switch  $S_{sm}$  comes to turn-OFF state. Then, both switched-inductor cells de-energizes and the voltage across the switched-inductor cells are equally delivers to load along with input voltage  $V_{in2}$ . The inductors in first cell  $L_{a1}$ ,  $L_{a2}$  are discharging and delivers energy towards the input voltage  $V_{in2}$  through switches  $S_{s2}$  along with diode  $D_{a3}$ . Also, the inductors in second cell  $L_{b1}$ ,  $L_{b2}$  are discharging and delivers energy towards the input voltage  $V_{in2}$  through switches  $S_{s2}$  along with diode  $D_{b3}$ . Accordingly, the currents of switched inductor cells  $I_{La1}$ ,  $I_{La2}$ ,  $I_{Lb1}$ ,  $I_{Lb2}$  input current  $I_{in2}$  flows continuously to meet load requirement and also charging the DC-link capacitor  $C_o$ . Thus, the current flow to load through output diode  $D_o$  because of forward bias to make series discharging of switched-inductor cells and obtains high voltage boost competency at load terminals. Then, the DC-link capacitor  $C_o$  stores energy continuously until switches  $S_{s1}$  and  $S_{sm}$  comes to turned-ON state. The mode-3 operation of SIMIDCBC topology is shwon in Figure 5(c). The typical waveforms of proposed SIMIDCBC topology is shown in Figure 6.

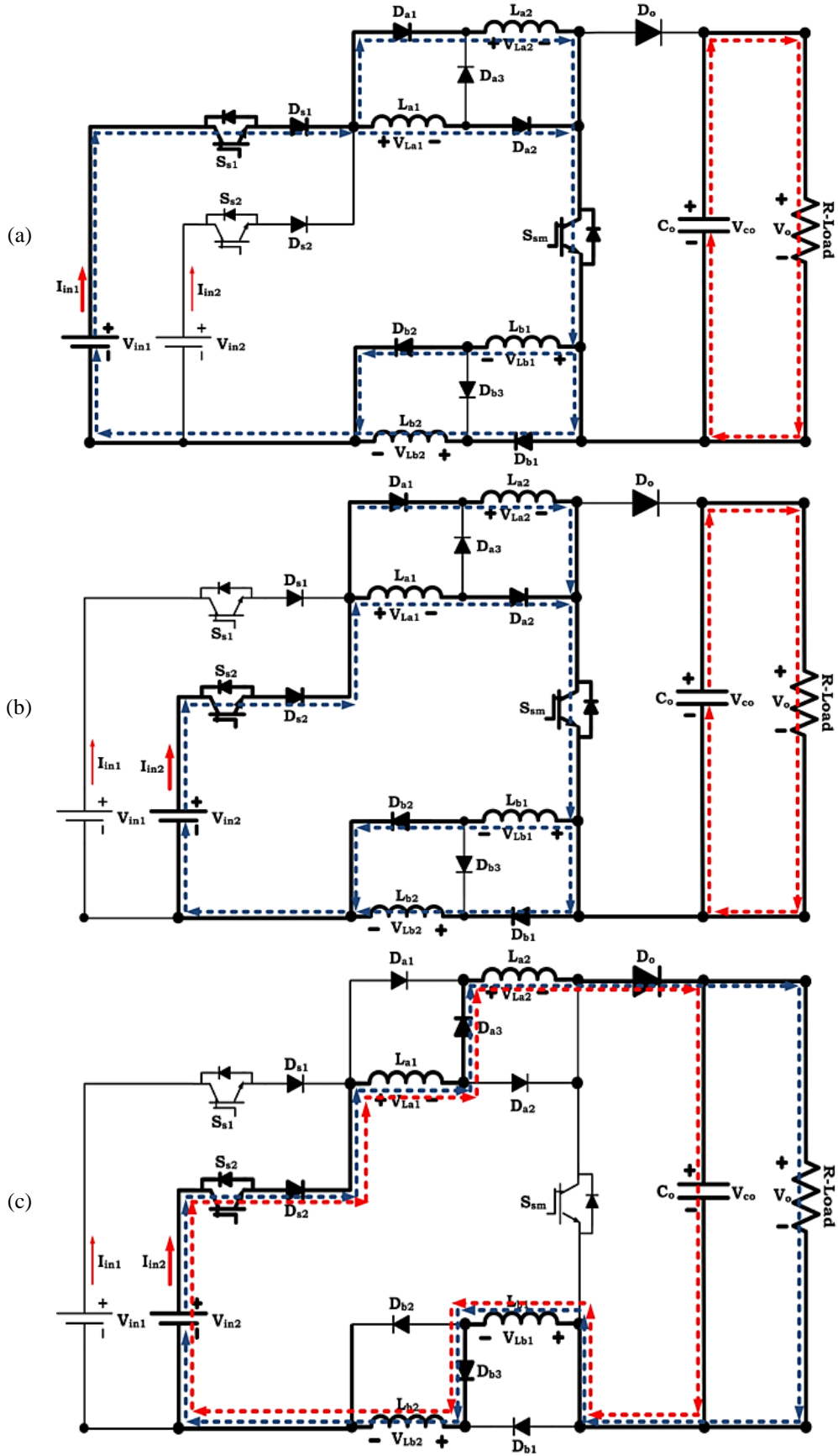


Figure 5. Operating modes (a) mode-1, (b) mode-2, and (c) mode-3

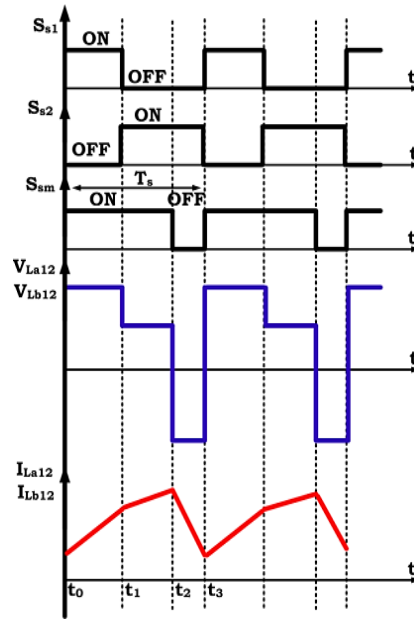


Figure 6. Typical waveforms

## 2.2. Steady-state analysis of SIMIDCBC topology

The average value of voltage induced in the switched-inductors are represented as:

$$V_{La12} = V_{Lb12} = 0 \quad (1)$$

During mode-1, the voltage induced and current flow in the switched inductors are formulated as:

$$V_{La12} = V_{Lb12} = V_{in1} \quad (2)$$

$$I_{La12}(t) = I_{Lb12}(t) = \frac{V_{in1}}{L} \quad (3)$$

During mode-2, the voltage induced and current flow in the switched inductors are formulated as:

$$V_{La12} = V_{Lb12} = V_{in2} \quad (4)$$

$$I_{La12}(t) = I_{Lb12}(t) = \frac{V_{in2}}{L} \quad (5)$$

Therefore, the dual input voltages are delivered equally through both switched-inductor cells due to equal values and are interfaced in series in mode-1 and mode-2. In mode-3, the voltage induced and current flow in the switched inductors are formulated as:

$$V_{La12} = V_{Lb12} = \frac{(V_{in2} - V_o)}{4} \quad (6)$$

$$I_{La12}(t) = I_{Lb12}(t) = \frac{(V_{in2} - V_o)}{4 * L} \quad (7)$$

Finally, volt-sec balance technique is applied, the voltage gain ( $V_{G_{CCM}}$ ) of SIMIDCBC topology is consistently depends on duty cycle of switches and the equation of voltage gain is formulated as (8).

$$V_{in1}D_{Ss1} + V_{in2}(D_{Ssm} - D_{Ss2}) + \frac{1}{4}(V_{in2} - V_o) \cdot (1 - D_{Ssm}) = 0 \quad (8)$$

Where,  $D_{Ss1}$ ,  $D_{Ss2}$ ,  $D_{Ssm}$  are the duty cycle's of switches  $S_{s1}$ ,  $S_{s2}$ ,  $S_{sm}$ , respectively. In (8) can be simplified and the final voltage gain ( $V_{G_{CCM}}$ ) is represented in (9).

$$VG_{CCM}(boost) = \frac{V_o}{V_{in}} = \frac{4D_{Ss2}(V_{in1}-V_{in2})+V_{in2}(1+D_{Ssm})}{(1-D_{Ssm})} \quad (9)$$

The switching pattern of VSI structure for PMSM drive is illustrated in Table 1. For controlling the rotor speed of PMSM drive, a vector-oriented control strategy has been adopted by sensing the actual speed and rotor position through hall-effect sensors  $H_a$ ,  $H_b$ , and  $H_c$ . At first, the actual speed  $N_a$  is extracted and compared with reference speed  $N_r^*$  which delivers some error sequences. These sequences are reduced by using proportional-integral (PI) controller and generates the  $I_d^*$  current in d-frame and also  $I_q^*$  is considered as zero. The extracted reference currents  $I_{dq}^*$  in dq-frame is transformed into standard reference current  $I_{abc}^*$  in abc-frame by using inverse-park's transformation technique. The reference current  $I_{abc}^*$  is compared with actual currents  $I_{abc}$  and the final outcome is delivered to SPWM which produces the feasible switching states to VSI structure. By switching the VSI structure, the stator windings of PMSM produces the required torque with the rotor position which produces the reference speed of PMSM drive.

Table 1. Switching pattern of VSI structure for PMSM drive

Switching angles	Switch pattern	Phase sequence			Hall-effect sensors			Turn-on switches	
		Emf.a	Emf.b	Emf.c	Ha	Hb	Hc		
0°~60°	$S_{p1}$	+ve	-ve	0	1	0	0	$S_{a1}$	$S_{a6}$
60°~120°	$S_{p2}$	+ve	0	-ve	1	1	0	$S_{a1}$	$S_{a2}$
120°~180°	$S_{p3}$	0	+ve	-ve	0	1	0	$S_{a2}$	$S_{a3}$
180°~240°	$S_{p4}$	-ve	+ve	0	0	1	1	$S_{a3}$	$S_{a4}$
240°~300°	$S_{p5}$	-ve	0	+ve	0	0	1	$S_{a4}$	$S_{a5}$
300°~360°	$S_{p6}$	0	-ve	+ve	1	0	1	$S_{a5}$	$S_{a6}$

### 3. RESULTS AND DISCUSSION

The performance of proposed SIMIDCBC topology driven PMSM for PEV application is verified under constant and variable speed conditions by using MATLAB/Simulink tool, simulation results are presented. The proposed SIMIDCBC topology is developed based on the desired output DC voltage with given input DC voltage through calculated system parameters is illustrated in Table 2.

Table 2. System parameters

S.No	System parameters	Values
1	Input and output DC voltage	$V_{in1}=40$ V, $V_{in2}=20$ V; $V_o=520$ V
2	Switched inductors and output capacitor	$L_{a1}=L_{a2}=L_{b1}=L_{b2}=1$ mH; $C_o=470$ $\mu$ F
3	Switching frequency	$F_s=20$ KHz
4	PMSM drive	$P_o=5$ KW, $N_r=3000$ rpm, $R_s=18.7$ $\Omega$ , $L_s=0.0268$ $\mu$ H, voltage constant ( $V_{peak} L-L/Krpm$ ) =63.48

#### 3.1. Performance evaluation of SIMIDCBC topology

The simulation results of proposed SIMIDCBC topology with dual inputs are shown in Figure 7 (see Appendix). The SIMIDCBC topology is powered with dual input voltages such as  $V_{in1}=40$  V and  $V_{in2}=20$  V for energizing the switched inductors to get required load voltage at load terminals as shown in Figure 7(a). Initially,  $V_{in1}=40$  V energizing the switched inductors during mode-1 and  $V_{in2}=20$  V energizing the switched inductors during mode-2 and mode-3. It produces the required load voltage of 520 V with a load current of 9.5 A to drive the R-load as shown in Figure 7(b). The both switched inductors cells are charged by turning-ON the respective switches through switching pulses generated by pulse-width modulation is depicted in Figure 7(c). However, the inductors in the cell are linearly charged by dual input DC sources,  $V_{in1}=40$  V energizing the switched inductors during mode-1 by using switches  $S_{s1}$  and  $S_{sm}$ , then the inductor current increased linearly in a positive-slope. Accordingly,  $V_{in2}=20$  V energizing the switched inductors during mode-2 and mode-3 by using switches  $S_{s2}$  and  $S_{sm}$ , then the inductor current increased linearly in a positive-slope with a inductor voltage of 18.5 V and the average current of 18.2 A as shown in Figures 7(d) and 7(e). The switches  $S_{s1}$  and  $S_{sm}$  are turned-ON in mode-1, thus no voltage is appeared across the switches and some voltage is appeared at switch  $S_{s2}$  which is equal to the  $V_{Ss1}-V_{Ss2}$  i.e. -20 V. Likewise, the switches  $S_{s2}$  and  $S_{sm}$  are turned-ON in mode-2, thus no voltage is appeared across the switches and some voltage is appeared at switch  $S_{s1}$  which is equal to the  $V_{Ss2}-V_{Ss1}$  i.e. 20 V. Similarly, the switch  $S_{sm}$  is turned-OFF in mode-3, thus some voltage is appeared across the switch is 520 V which is same as the voltage across the R-load with a maximum current flow through these switches is nearly 1A as shown in Figures 7(f) and 7(g). In mode-1, 2,

the diodes  $D_{a3}$ ,  $D_{b3}$  and  $D_o$  are in reverse bias, thus some voltage is appeared across the diodes is -17.5 V, -125 V, -520 V, respectively. The voltage across the  $D_o$  diode should varies based on the switching mode, the diodes  $D_{a1}$ ,  $D_{a2}$  and  $D_{b1}$ ,  $D_{b2}$  are reverse bias in mode-3 and some of voltage appeared across these diodes are measured as -125 V and -125 V is shown in Figures 7(h) and 7(i). Also, the maximum current flow through the diodes irrespective of switching modes is measured as 20 A is shown in Figures 7(j) and 7(k), respectively.

### 3.2. Performance evaluation of SIMIDCBC topology fed PMSM drive for PEV application under constant speed condition

The simulation results of proposed SIMIDCBC topology fed PMSM drive for PEV application under constant speed condition is shown in Figure 8. The PMSM drive is integrated at output of proposed SIMIDCBC topology by using 3-level VSI structure which produces the 3-level output voltage of 520 V and obtains sinusoidal stator current of 10 A which drives the output power of PMSM drive as 5 kW is shown in Figures 8(a) and 8(b). The rotor speed of PMSM drive obtains the constant rated speed of 3000 rpm which is achieved as per given reference speed as shown in Figure 8(c). During starting state, the PMSM drive provides the electromagnetic torque of 8 N-m and during steady-state condition the PMSM drive achieves the rated electromagnetic torque of 5 N-m to drive the load torque of 5 N-m for PEV application as shown in Figure 8(d). The rotor angle of PMSM drive is systematically sensed by Hall-effect sensors obtains the 6.28 rad/sec which represents the sequential switching of VSI for getting the clock-wise 360° direction of rotor as shown in Figure 8(e).

### 3.3. Performance evaluation of SIMIDCBC topology fed PMSM drive for PEV application under variable speed condition

The simulation results of proposed SIMIDCBC topology fed PMSM drive for PEV application under variable speed condition is shown in Figure 9. In this condition, the reference speed of PMSM drive is varied in the range of 2000 to 3500 rpm (incremental speed) and 3500 to 2000 rpm (decremental speed) with respect to time (0 sec < t < 0.7 sec). The PMSM drive is integrated at output of proposed SIMIDCBC topology by using 3-level VSI structure which produces the 3-level output voltage of 520 V and obtains constant and sinusoidal stator current of 10 A which drives the output power of PMSM drive as 5 kW is shown in Figures 9(a) and 9(b). The rotor speed of PMSM drive obtains the variable speed of 2000 to 3500 rpm which is achieved as per given reference speed as shown in Figure 9(c). During starting state, the PMSM drive provides the electromagnetic torque of 8 N-m and during steady-state condition the PMSM drive achieves the rated electromagnetic torque of 5 Nm to drive the load torque of 5 Nm for PEV application as shown in Figure 9(d). The rotor angle of PMSM drive is systematically sensed by Hall-effect sensors obtains the 6.28 rad/sec which represents the sequential switching of VSI for getting the clock-wise 360° direction of rotor as shown in Figure 9(e). The comparison of various conventional and proposed SIMIDCBC topologies is illustrated in Table 3. The proposed SIMIDCBC topology produces high boost voltage which is nearly 9 times of input DC voltage by using low switching elements over the conventional multi-port DC-DC converter topologies. The graphical view of voltage gain ( $M_{CCM}$ ) vs. duty ratio ( $D$ ) comparison of conventional boost converter and proposed SIMIDCBC DC-DC boost converter is shown in Figure 10.

Table 3. Comparison of various conventional and proposed SIMIDCBC topologies

Topology type	Voltage gain formula	Voltage gain	No. of input DC sources	No. of semi-conductors	Diodes	Inductor cell:	No. Of passive Elements	Capacitors
Basic DC-DC boost converter [8]	$V_0 = \frac{1}{(1-D)} V_{in}$	3 times	1	1	1	1	1	1
Multi-input DC-DC boost converter [23]]	$V_0 = \frac{1}{(1-D)} V_{in}$	3 times	3	4	7	1	3	
Three-port hybrid converter [24]	$V_0 = \frac{(1+D^2-D)}{(1-D)^2} V_{in}$	4 times	3	4	4	2	2	
Multi-input SEPIC converter [25]	$V_0 = \frac{1+D}{(1-D)^2} V_{in}$	5 times	2	3	5	3	2	
Proposed SIMIDCBC topology	$V_0 = \frac{4D_{ss2}(V_{in1} - V_{in2}) + V_{in2}(1 + D_{ssm})}{(1 - D_{ssm})} V_{in}$	9 times	2	3	8	2	1	



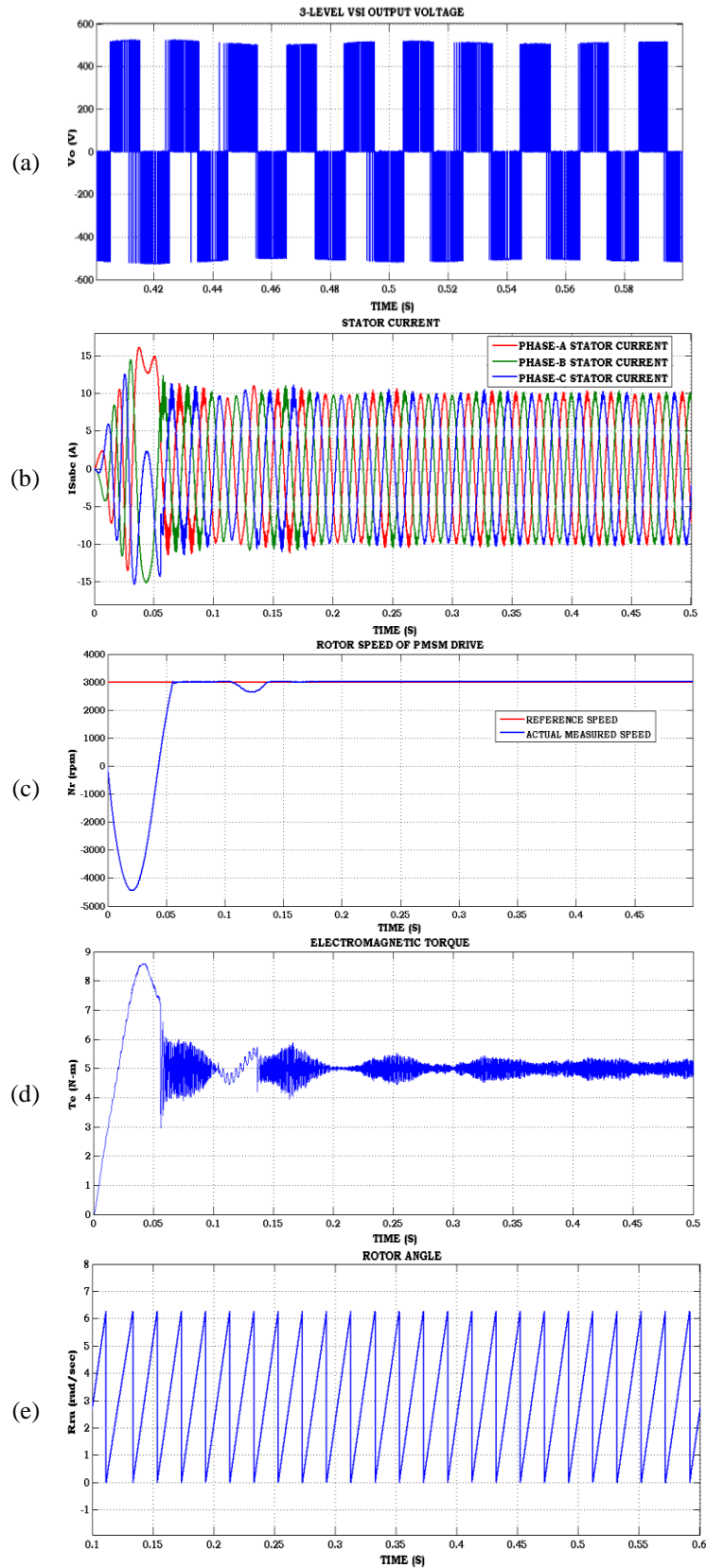


Figure 8. Simulation results of proposed SIMIDCBC topology fed PMSM drive for PEV application under constant speed condition (a) output voltage of 3-level VSI structure, (b) stator current of PMSM drive, (c) rotor speed of PMSM drive, (d) electromagnetic torque of PMSM drive, and (e) rotor angle measurement of PMSM drive

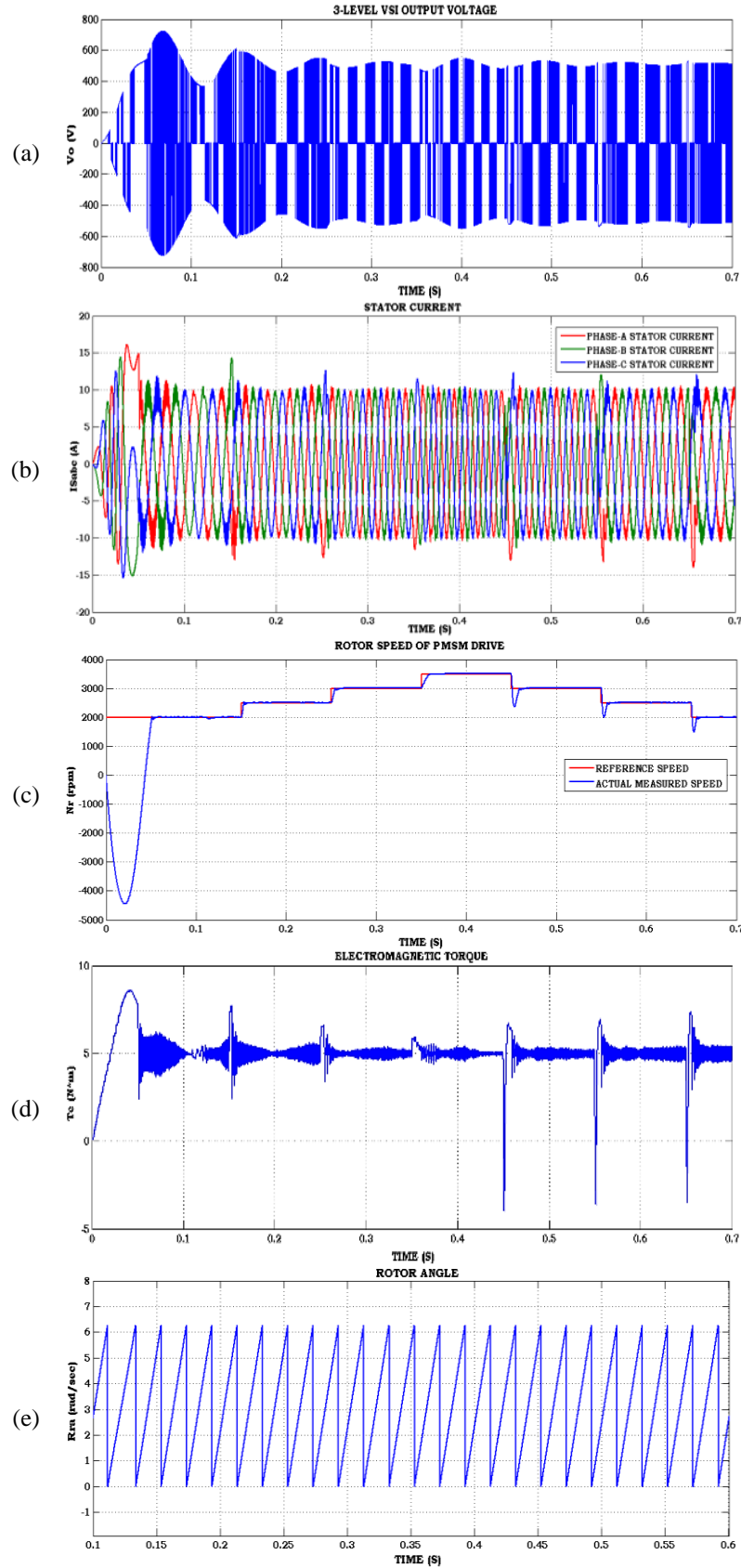


Figure 9. Simulation results of proposed SIMIDCBC topology fed PMSM drive for PEV application under variable speed condition (a) output voltage of 3-level VSI structure, (b) stator current of PMSM drive, (c) rotor speed of PMSM drive, (d) electromagnetic torque of PMSM drive, and (e) rotor angle measurement of PMSM drive

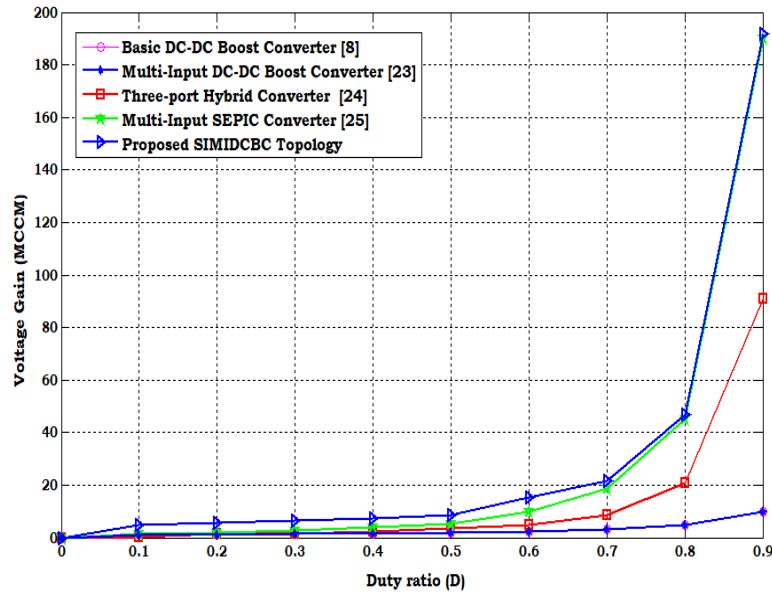


Figure 10. Graphical view

#### 4. CONCLUSION

In this work, a two-input single-output switched-inductor type DC-DC boost converter for combined energy sources for PEV application is presented. The proposed SIMIDCBC topology requires only three switches; two switched inductor cells. The voltage gain of proposed SIMIDCBC topology is higher than conventional DC-DC boost converter topologies. The proposed SIMIDCBC topology have good features such as efficient operation, reliable performance, continuous input current, low  $dv/dt$  stress, low ripple current and enables the acceptable configuration for combined integration of multiple energy sources to drive the EV system. The performance of proposed SIMIDCBC topology driven PMSM for PEV application under constant and variable speed condition is verified by using MATLAB/Simulink tool, simulation results are presented.

#### APPENDIX

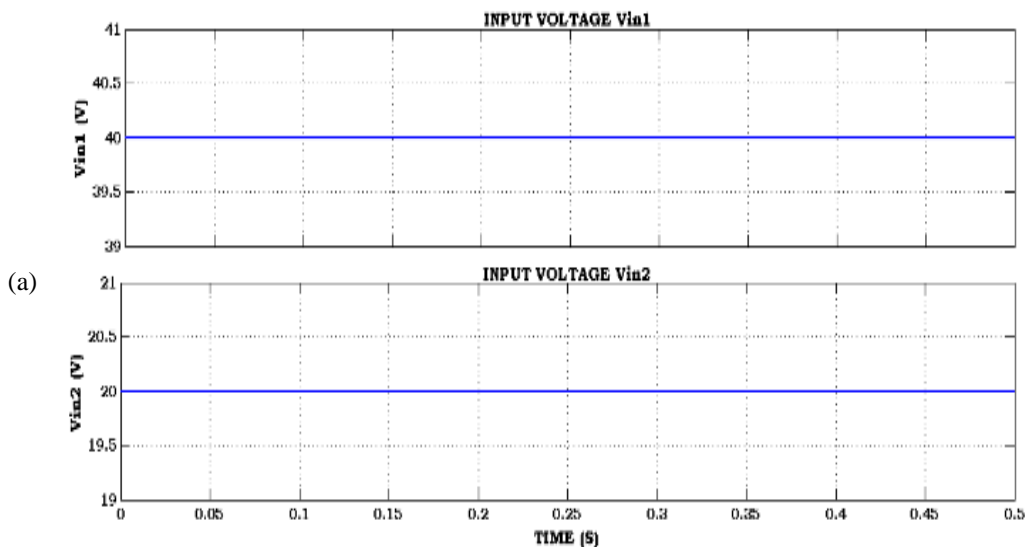


Figure 7. Simulation results of proposed SIMIDCBC topology with dual inputs: (a) input DC voltages

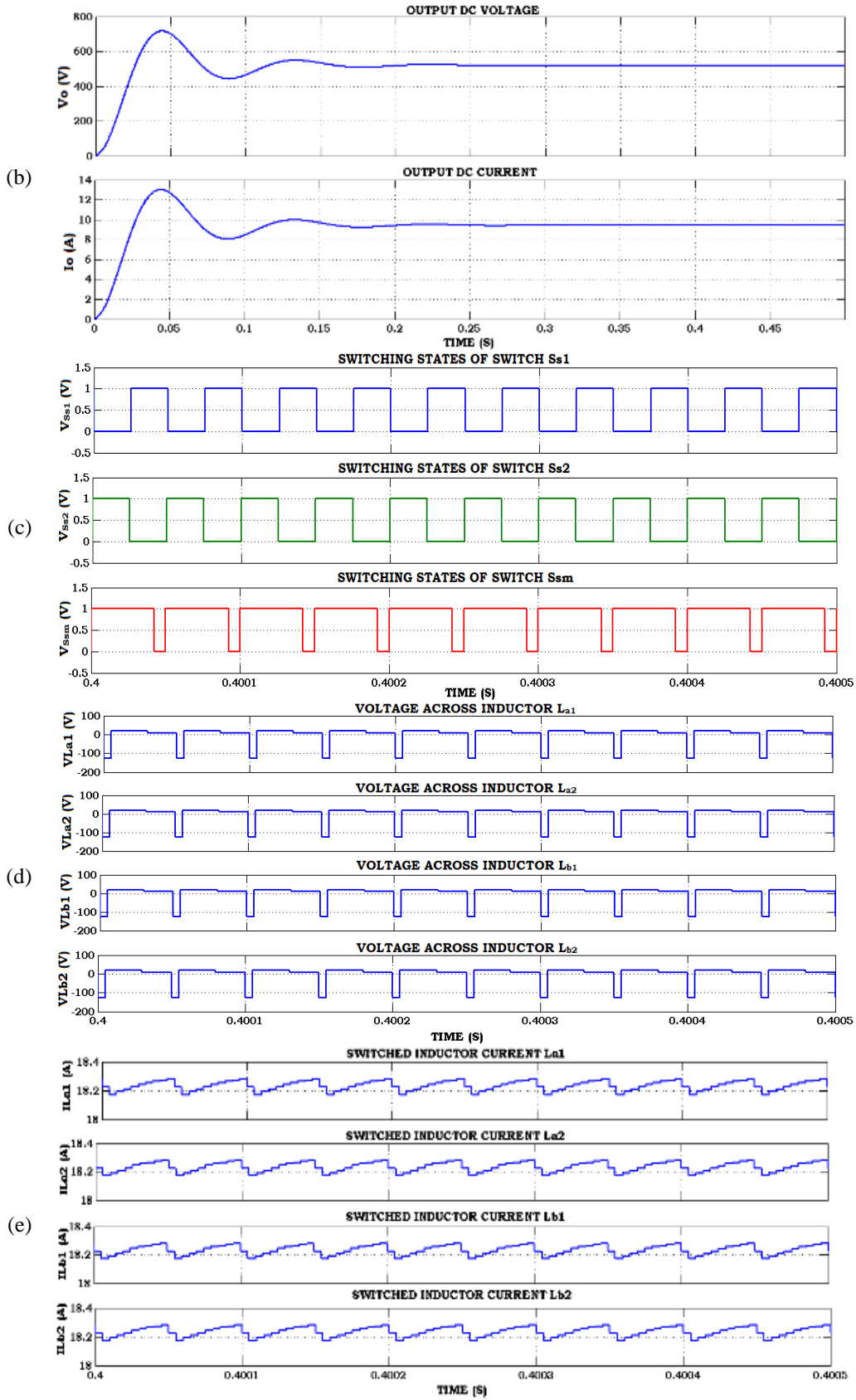


Figure 7. Simulation results of proposed SIMIDCBC topology with dual inputs: (b) output DC voltage and current, (c) switching states, (d) voltage across at switched-inductors, and (e) current flow in switched inductors (continue)

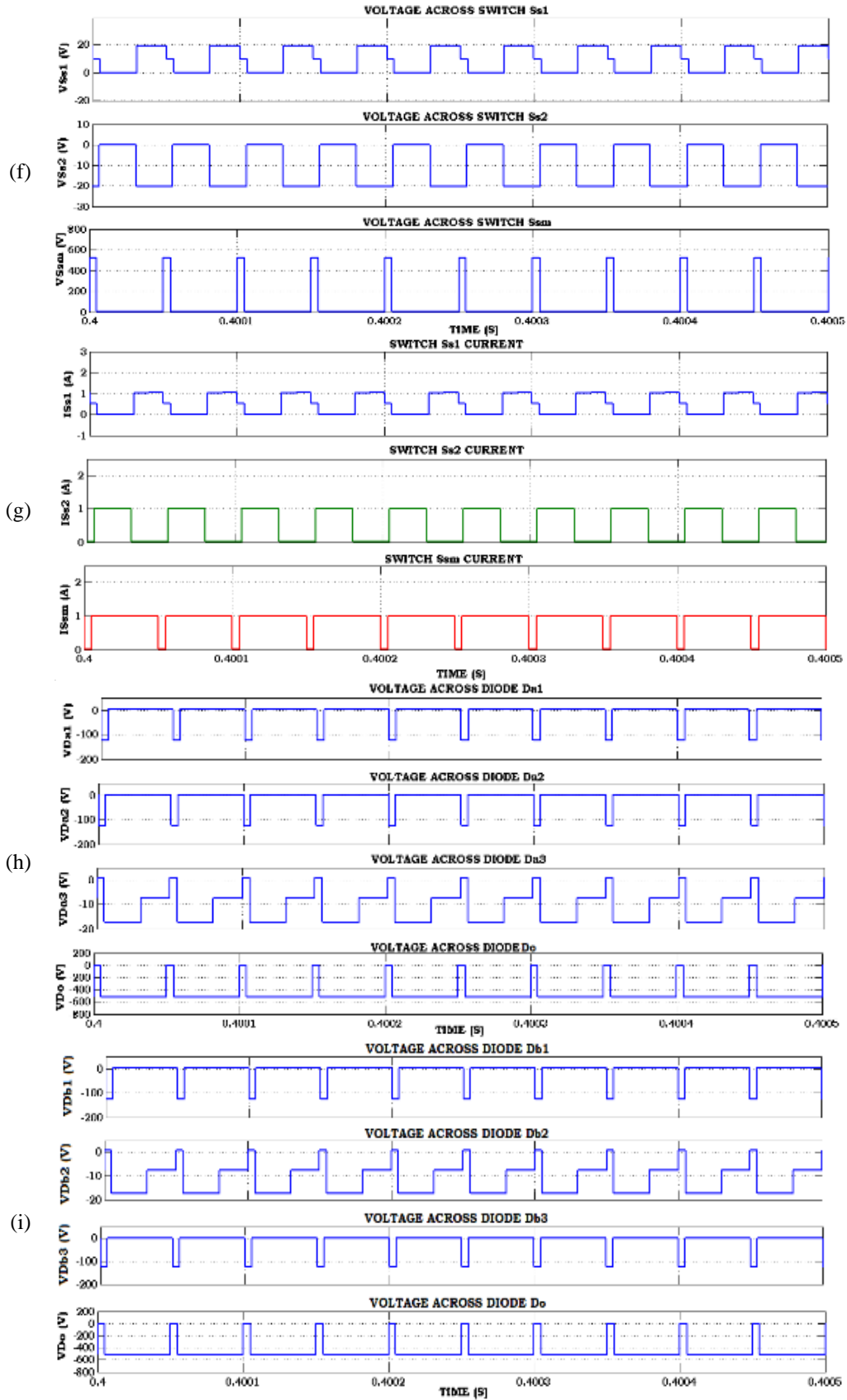


Figure 7. Simulation results of proposed SIMIDCBC topology with dual inputs: (f) voltage across at switches, (g) current flow in switches, (h) voltage across diodes-A, and (i) voltage across at diodes-B (continue)

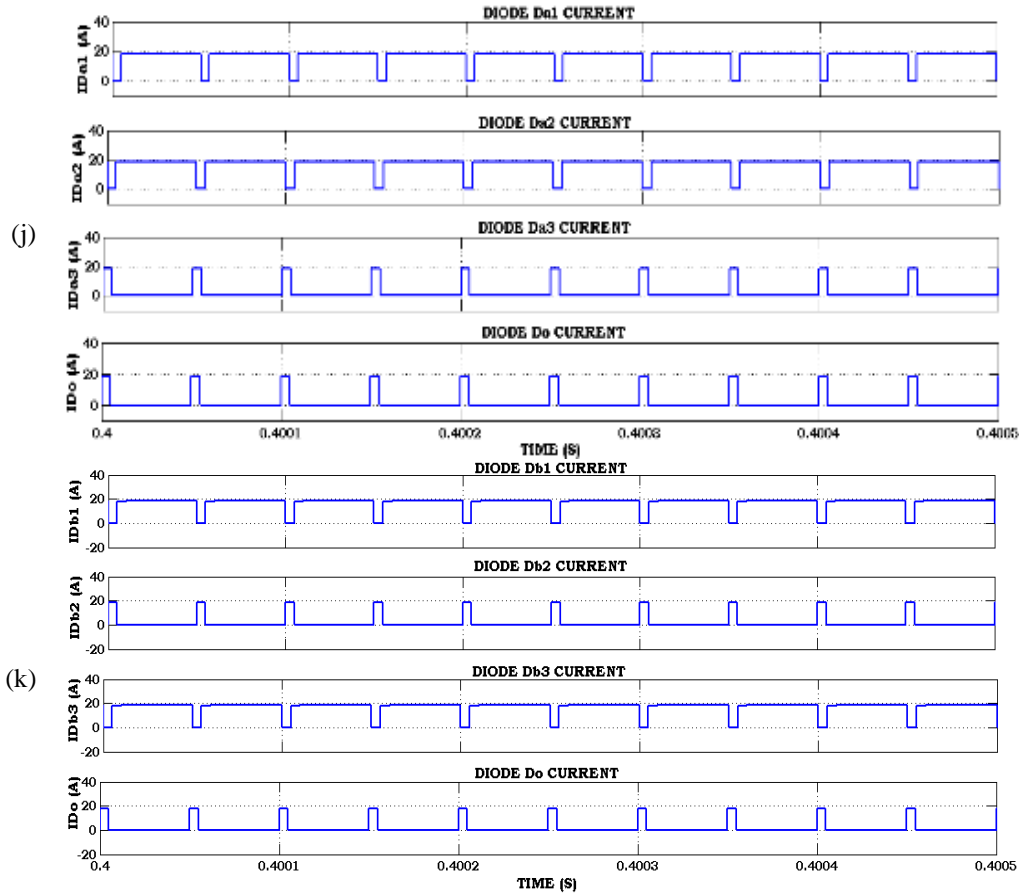


Figure 7. Simulation results of proposed SIMIDCBC topology with dual inputs: (j) current flow in diodes-A and (k) current flow in diodes-B (continue)





## REFERENCES

- [1] I. Husain *et al.*, "Electric drive technology trends, challenges, and opportunities for future electric vehicles," *Proceedings of the IEEE*, vol. 109, no. 6, pp. 1039–1059, Jun. 2021, doi: 10.1109/JPROC.2020.3046112.
- [2] B. MacInnis and J. A. Krosnick, "Climate Insights 2020: Surveying American Public Opinion on Climate Change and the Environment," *Resources for the Future and Stanford University*, 2020. [www.rff.org/climateinsights](http://www.rff.org/climateinsights)
- [3] S. J. Rind, Y. Ren, Y. Hu, J. Wang, and L. Jiang, "Configurations and control of traction motors for electric vehicles: A review," *Chinese Journal of Electrical Engineering*, vol. 3, no. 3, pp. 1–17, Dec. 2017, doi: 10.23919/CJEE.2017.8250419.
- [4] J. C. Gomez and M. M. Morcos, "Impact of EV battery chargers on the power quality of distribution systems," *IEEE Transactions on Power Delivery*, vol. 18, no. 3, pp. 975–981, Jul. 2003, doi: 10.1109/TPWRD.2003.813873.
- [5] K. J. Dyke, N. Schofield, and M. Barnes, "The impact of transport electrification on electrical networks," *IEEE Transactions on Industrial Electronics*, vol. 57, no. 12, pp. 3917–3926, Dec. 2010, doi: 10.1109/TIE.2010.2040563.
- [6] O. N. Nezamuddin, C. L. Nicholas, and E. C. dos Santos, "The problem of electric vehicle charging: state-of-the-art and an innovative solution," *IEEE Transactions on Intelligent Transportation Systems*, vol. 23, no. 5, pp. 4663–4673, May 2022, doi: 10.1109/TITS.2020.3048728.
- [7] M. H. Mobarak, R. N. Kleiman, and J. Bauman, "Solar-charged electric vehicles: a comprehensive analysis of grid, driver, and environmental benefits," *IEEE Transactions on Transportation Electrification*, vol. 7, no. 2, pp. 579–603, Jun. 2021, doi: 10.1109/TTE.2020.2996363.
- [8] M. Safayatullah, M. T. Elrais, S. Ghosh, R. Rezaii, and I. Batarseh, "A comprehensive review of power converter topologies and control methods for electric vehicle fast charging applications," *IEEE Access*, vol. 10, pp. 40753–40793, 2022, doi: 10.1109/ACCESS.2022.3166935.
- [9] C. Sain, P. K. Biswas, P. R. Satpathy, T. S. Babu, and H. H. Alhelou, "Self-controlled PMSM drive employed in light electric vehicle-dynamic strategy and performance optimization," *IEEE Access*, vol. 9, pp. 57967–57975, 2021, doi: 10.1109/ACCESS.2021.3072910.
- [10] R. Wang, X. Jia, S. Dong, and Q. Zhang, "PMSM driving system design for electric vehicle applications based on bi-directional quasi-Z-source inverter," in *2018 13th IEEE Conference on Industrial Electronics and Applications (ICIEA)*, IEEE, May 2018, pp. 1733–1738, doi: 10.1109/ICIEA.2018.8397989.
- [11] Y. Bai, J. Li, H. He, R. C. Dos Santos, and Q. Yang, "Optimal design of a hybrid energy storage system in a plug-in hybrid electric vehicle for battery lifetime improvement," *IEEE Access*, vol. 8, pp. 142148–142158, 2020, doi: 10.1109/ACCESS.2020.3013596.
- [12] E. Taherzadeh, H. Radmanesh, and A. Mehrizi-Sani, "A comprehensive study of the parameters impacting the fuel economy of plug-in hybrid electric vehicles," *IEEE Transactions on Intelligent Vehicles*, vol. 5, no. 4, pp. 596–615, Dec. 2020, doi: 10.1109/TIV.2020.2993520.
- [13] Y.-C. Liu and Y.-M. Chen, "A systematic approach to synthesizing multi-input DC–DC converters," *IEEE Transactions on Power Electronics*, vol. 24, no. 1, pp. 116–127, Jan. 2009, doi: 10.1109/TPEL.2008.2009170.





- [14] R.-J. Wai and B.-H. Chen, "High-efficiency dual-input interleaved DC–DC converter for reversible power sources," *IEEE Transactions on Power Electronics*, vol. 29, no. 6, pp. 2903–2921, Jun. 2014, doi: 10.1109/TPEL.2013.2275663.
- [15] A. Khaligh, Jian Cao, and Young-Joo Lee, "A multiple-input DC–DC converter topology," *IEEE Transactions on Power Electronics*, vol. 24, no. 3, pp. 862–868, Mar. 2009, doi: 10.1109/TPEL.2008.2009308.
- [16] S. H. Hosseini, S. K. Haghighian, S. Danyali, and H. Aghazadeh, "Multi-input DC boost converter supplied by a hybrid PV/Wind turbine power systems for street lighting application connected to the grid," in *2012 47th International Universities Power Engineering Conference (UPEC)*, IEEE, Sep. 2012, pp. 1–6. doi: 10.1109/UPEC.2012.6398632.
- [17] A. Kwasinski and P. T. Krein, "A microgrid-based telecom power system using modular multiple-input DC-DC converters," in *INTELEC 05 - Twenty-Seventh International Telecommunications Conference*, IEEE, Sep. 2005, pp. 515–520. doi: 10.1109/INTELEC.2005.335152.
- [18] R.-J. Wai, C.-Y. Lin, and B.-H. Chen, "High-efficiency DC–DC converter with two input power sources," *IEEE Transactions on Power Electronics*, vol. 27, no. 4, pp. 1862–1875, Apr. 2012, doi: 10.1109/TPEL.2011.2170222.
- [19] J. Lam and P. K. Jain, "A novel electrolytic capacitor-less multi-input DC/DC converter with soft-switching capability for hybrid renewable energy system," in *2014 16th European Conference on Power Electronics and Applications*, IEEE, Aug. 2014, pp. 1–10. doi: 10.1109/EPE.2014.6911040.
- [20] A. Nahavandi, M. T. Hagh, M. B. B. Sharifian, and S. Danyali, "A nonisolated multiinput multioutput DC–DC boost converter for electric vehicle applications," *IEEE Transactions on Power Electronics*, vol. 30, no. 4, pp. 1818–1835, Apr. 2015, doi: 10.1109/TPEL.2014.2325830.
- [21] S. K. Haghighian, S. Tohidi, M. R. Feyzi, and M. Sabahi, "Design and analysis of a novel SEPIC-based multi-input DC/DC converter," *IET Power Electronics*, vol. 10, no. 12, pp. 1393–1402, Oct. 2017, doi: 10.1049/iet-pel.2016.0654.
- [22] F. Akar, Y. Tavlasoglu, E. Ugur, B. Vural, and I. Aksoy, "A bidirectional nonisolated multi-input DC–DC converter for hybrid energy storage systems in electric vehicles," *IEEE Transactions on Vehicular Technology*, vol. 65, no. 10, pp. 7944–7955, Oct. 2016, doi: 10.1109/TVT.2015.2500683.
- [23] E. Babaei and O. Abbasi, "Structure for multi-input multi-output DC–DC boost converter," *IET Power Electronics*, vol. 9, no. 1, pp. 9–19, Jan. 2016, doi: 10.1049/iet-pel.2014.0985.
- [24] F. Kardan, R. Alizadeh, and M. R. Banaei, "A new three input DC/DC converter for hybrid PV/FC/battery applications," *IEEE Journal of Emerging and Selected Topics in Power Electronics*, vol. 5, no. 4, pp. 1771–1778, Dec. 2017, doi: 10.1109/JESTPE.2017.2731816.
- [25] K. V. K. Varma and A. Ramkumar, "Implementation of SPV-powered water pumping system using non-isolated SC converter topology," *Electrical Engineering*, vol. 103, no. 3, pp. 1433–1444, Jun. 2021, doi: 10.1007/s00202-020-01170-9.
- [26] A. Sanam, L. S. Rao, R. Kommineni, S. Shaik, V. Regulagadda, and G. S. Doddi, "A solar-PV/BESS powered multi-input DC-DC boost converter fed BLDC motor drive," in *2022 International Conference on Intelligent Controller and Computing for Smart Power (ICICCSPP)*, IEEE, Jul. 2022, pp. 1–6. doi: 10.1109/ICICCSPP53532.2022.9862420.

## BIOGRAPHIES OF AUTHORS







**Chinta Anil Kumar**     currently research scholar in Department of Electrical and Electronics Engineering at Annamalai University, Annamalai Nagar, India. He has done B.Tech. in Electrical and Electronics Engineering from Acharya Nagarjuna University, Guntur, Andhra Pradesh, India and M.Tech. in Power Electronics and Drives from Vignan University, Guntur, Andhra Pradesh, India. His main research areas include renewable energy integration and electrical vehicles. He can be contacted at email: chanilkumar.eee@gmail.com.



**Kandasamy Jothinathan**     currently working as professor with the Department of Electrical and Electronics Engineering at Annamalai university, Annamalai Nagar, India. He received the BE degree Electrical and Electronics Engineering and the ME degree in power system from Annamalai university. He received Ph.D. degree in the year of 2017 from Annamalai University, Annamalai Nagar. His research topic includes power system operation and control, security analysis. He can be contacted at email: jothi.eeau@yahoo.com.



**Lingineni Shanmukha Rao**     received Ph.D., from Jawaharlal Nehru Technological University Hyderabad (JNTUH), Hyderabad, India in 2016 and M.Tech., in Electrical Power Engineering from Jawaharlal Nehru Technological University (J.N.T.U), Hyderabad, A.P, India in 2006. At Present he is working as Professor and Head of the Department Electrical and Electronics Engineering at Kallam Haranadhareddy Institute of Engineering & Technology, Guntur, A.P., India. He authored four books and published more than 27 research papers in international journals and conferences. His research interests include power system modeling and control, renewable energy sources and soft computing techniques. He can be contacted at mail: lsrlingineni@gmail.com.